

# The World's Worst Roads— What Are Their Profiles?

Herbert E. Lindberg  
Owner, LCE Science/Software  
Penn Valley, California  
(530) 432-5096

A convex model of uncertainty based on a Fourier transform description of road roughness is used with the same systematic variation of roughness with wavelength that was measured for probabilistic analyses. This variation, together with a separate but very simple bounding measurement, allows calculation of reasonable estimates of maximum accelerations and maximum displacements for a range of motor vehicle parameters. Road profiles that lead to these undesirable responses are also found. These are recommended for use by road builders as profiles to be avoided during standard road construction, and profiles to be included in test track construction to ensure critical testing. All these results are obtained without need for assumed probability distributions of road roughness, which are most questionable in the tails needed for high-confidence maximum response estimates by probabilistic methods.

## WHY CONVEX MODELING?

A rough road that causes discomfort and vehicle stress is like pornography: we all recognize it when we see it, but it is very difficult to define. Previous analyses focused on power spectral density of vehicle acceleration as a measure of discomfort, but left open the question of road profiles that cause discomfort. Also, while it is possible with probabilistic models of uncertainty to calculate at a specified confidence level the maximum acceleration one is not likely to exceed, the calculation requires knowledge of the probability distribution of road roughness. Obtaining this knowledge is elusive for high confidence levels because the tail of the distribution is difficult to measure and assumed distributions are open to question.

Convex modeling addresses these shortcomings of probabilistic response analysis. In the following it is shown that a convex model based on a Fourier transform description of road roughness gives reasonable estimates of maximum accelerations (or displacements) without such questions. By reasonable we mean that the estimates are conservative by virtue of the method used to calculate them, but not overly conservative because the knowledge of roughness variations with wavelength is used to its fullest. Furthermore, specific road profiles that give maximum accelerations or maximum displacements in any given vehicle are also calculated — the nature of truly rough roads is revealed. These are recommended for use by road builders as profiles to be avoided during standard road construction, and profiles to be included in test track construction to ensure critical testing.

In the remainder of the paper we first review the established method for describing road roughness from the view needed for the Fourier convex model. Then dynamic response analysis is presented of a simple vehicle model used to demonstrate convex modeling, followed by the convex model and its solution. Numerical results are given for maximum acceleration and maximum displacement responses as functions of vehicle model parameters. For selected parameters, worst-road profiles are plotted to show the features of the world's worst roads.

## DESCRIPTION OF ROAD ROUGHNESS

Estimates of vehicle response over a broad class of roads have been based on spectral descriptions of road roughness presented in [3] (Dodds and Robson, 1973). The most widely used are those given in [8] (Robson, 1979), where the power spectral density of roughness, based on measurements of a wide variety of road surfaces, is specified by

$$S(\nu) = \begin{cases} k\nu^{-2.5} & 0.01 \leq \nu \leq 10 \\ k(0.01)^{-2.5} & 0 < \nu < 0.01 \end{cases} \quad (1)$$

where  $\nu$  is wave number in cycles/m, and coefficient  $k$ , in units  $\text{m}^{0.5}$ , was determined as follows for  $S(\nu)$  in  $\text{m}^2/(\text{cycles/m})$ :

$$\begin{array}{lll} 3 \times 10^{-8} < k < 50 \times 10^{-8} & \bar{k} = 10 \times 10^{-8} & \text{motorways (freeways)} \\ 3 \times 10^{-8} < k < 800 \times 10^{-8} & \bar{k} = 50 \times 10^{-8} & \text{main roads} \\ 50 \times 10^{-8} < k < 3000 \times 10^{-8} & \bar{k} = 500 \times 10^{-8} & \text{minor roads} \end{array}$$

The range of  $\nu$  over which  $S(\nu)$  is defined in equation (1) will be discussed later in this section.

In [8] and work by Sharp and Aly Hassan ([12], 1984) and others,  $S(\nu)$  is the power spectral density of road roughness considered as random deviations from perfect flatness. This leads to random vibrations of vehicles traversing such roads. Typically,  $S(\nu)$  is used together with vehicle dynamic equations of motion from which transfer functions are derived for quantities of interest. These allow calculation of the power spectral densities of quantities such as vehicle body acceleration and displacement, wheel-body displacement, and even passenger seat motion in detailed models.

In theory, these densities and the assumption that road roughness spectral amplitudes are uncorrelated and have a normal (Gaussian) probability distribution can also be used to calculate maximum accelerations or displacements for specified confidence levels. However, this is seldom done. An early procedure for estimating ride comfort was to compare calculated curves of acceleration power density versus frequency with empirically derived curves in [13] (Van Deusen, 1968) for subjective comfort limits. This evolved into weighting the calculated response spectra by empirical spectra for discomfort ([5], ISO 2631, 1983, and [12], Sharp and Aly Hassan, 1984).

These ride comfort evaluations implicitly envision road profiles as a sequence of washboards at single wavelengths, with little consideration of the superposition effects of simultaneous excitation by the broad spectrum of wavelengths that comprise road roughness. We all know from experience that another form of discomfort comes from traversing a section of rough road that builds up large accelerations or displacements, followed by a more quiescent state. It is shown here that road profiles that produce such response are not single-wavelength washboards at vehicle resonance, but comprise many wavelengths that excite the complete spectrum of vehicle response. It is important to consider such road profiles because the vehicle response spectrum integrates the road roughness power spectral density over a broad range of frequencies, especially for the well-damped broad spectra of engineered suspension systems.

The present analysis addresses these superposition effects by using the spectral distribution of road roughness in a completely different way. We begin by reviewing the definition of  $S(\nu)$ . Consider a length of road,  $L$ , long enough to represent all wavelengths of interest. Just how long this must be will become clear. Consider also a single wavelength  $\ell$  corresponding to wave number  $\nu = 1/\ell$ . The number of such waves in length  $L$  is  $n = L/\ell$ , where  $\nu = n/L$  is taken such that  $n$  is an integer. The road profile for this component of roughness is

$$\delta_n(x) = c_n \cos\left(\frac{2\pi nx}{L} + \beta_n\right) \quad (2)$$

where  $x$  is distance along the road,  $c_n$  is the component amplitude in meters, and  $\beta_n$  is the phase shift of the wave relative to the  $x$  origin. (In random noise theory it is more usual to express the wave in terms of its cosine and sine parts, of amplitudes  $a_n$  and  $b_n$ , but the above form is equivalent and more directly applicable to the use of  $S(\nu)$  that follows.)

When a vehicle traverses the road at velocity  $V$ , then  $x = Vt$ , where  $t$  is time, so the motion at contact with the road is

$$\delta_n(t) = c_n \cos\left(\frac{2\pi nVt}{L} + \beta_n\right) \quad (3)$$

and the excitation frequency is  $\omega_n = 2\pi nV/L$  radians/s or  $f_n = nV/L = \nu V$  cps.

The *power* of this component is  $c_n^2/2$ , from the analogy to a sinusoidal electric current of amplitude  $c_n$  amperes flowing through a one-watt resistor [the origin of the terminology *power spectral density*  $S(f)$ ]. From the definition of  $S(f)$ , the power at frequency  $f$  is  $S(f)df$ . On the interval  $0, L$  we have  $f \Rightarrow f_n$  and  $df \Rightarrow f_{n+1} - f_n = V/L$ , and hence  $c_n^2/2 = S(f)V/L$ . With  $S$  expressed as  $S(\nu)$ , the power at  $\nu$  is  $S(\nu)d\nu = S(\nu)/L$ . Thus,

$$c_n^2 = \frac{2S(\nu)}{L} = 2kL^{1.5}n^{-2.5} \quad (4)$$

Vehicles for which  $S(\nu)$  is applied have frequencies of interest ranging from 0.5 Hz (a suitable fraction of the lowest body-dominated frequency, of a large luxury automobile) to 50 Hz (a suitable multiple of the highest wheel bounce frequency, of a small economy automobile). Velocities of concern range from about 5 to 50 m/s (18 to 180 km/hr, about 11 to 112 mph). With  $\nu = f/V$  from the above discussion, the smallest wave number of concern is  $\nu = 0.5/50 = 0.01$ , and the largest is  $\nu = 50/5 = 10$ , which are the values used in equation (1). The straight line fit to a log-log plot of measured data was centered in this range to obtain the exponent  $-2.5$  given in this equation. Data outside this range were considered to be of secondary concern. The constant value of  $S(\nu)$  given in equation (1) for lower wave numbers is a convenience to avoid inordinately large roughness amplitudes if the  $-2.5$  exponent were applied in this range, and reflects to a reasonable extent that very long wavelength roughness amplitudes vary more slowly with wavelength, in addition to being difficult to measure.

Finally, the lowest wave number of concern influences the interval length  $L$  to be used in the finite Fourier transform analysis in this paper. Thus, to include a wave number of 0.01 cycles/m,  $L$  must be at least the 100 meters of the corresponding wavelength. In measurements for determining  $S(\nu)$ , the road sections to be measured must be much longer than 100 meters to include a representative sample of waves of length 100 meters. Another consideration for  $L$  is the resolution desired for  $\nu$ , since  $\Delta\nu = 1/L$ , which again indicates a value substantially larger than 100 meters to adequately resolve wave numbers near the 0.01 lower limit. In any specific analysis,  $L$  should be from five to ten times the wavelength for the lowest frequency and highest velocity of the automobile-road combination being analyzed.

The total excitation from the road profile is the sum of the Fourier components given by equation (3). With

$$\theta = 2\pi Vt/L \quad (5)$$

introduced for convenience, the total excitation is

$$\delta(t) = \sum_{n=1}^N c_n \cos(n\theta + \beta_n) \quad (6)$$

Observe that, as  $\theta$  ranges from 0 to  $2\pi$ , the vehicle moves from  $x = 0$  to  $x = Vt = L$ . Thus, in the following finite transform analysis over the interval  $0, L$  it is helpful to envision that the vehicle moves around a circular test track of length  $L$ . The upper limit  $N$  is the highest mode number that leads to significant dynamic response.

## VEHICLE DYNAMICS

In this paper the simplest possible representation of a motor vehicle is used, to illustrate application of convex modeling with a minimum of parameters and complexity. This representation is a one degree-of-freedom model consisting of the main body mass  $m$  supported by a suspension spring  $K$  that rides on the road surface, plus a viscous damper  $C$  in parallel with  $K$ . Even with this oversimplified model, the results are useful in characterizing worst-road profiles as they affect main vehicle body acceleration and hence ride comfort, as well as suspension displacement and hence space requirements.

Such a 1-dof model has been used by others in preliminary analyses, as in [9] (Ryba, 1973), but most analyses have been done with a *quarter car* model, which is a 2-dof model that includes the elements of the 1-dof model plus an unsprung wheel mass and an associated tire spring that rides on the road surface. In [11] (Sharp and Crolla, 1987) and [12] (Sharp and Aly Hassan, 1984) it is demonstrated that this model is suitable for all but the most exacting evaluations of specific automobile designs, for example with 6-dof models that include pitch and roll, or by FEM analysis.

Transfer functions for the quarter car model are given in [10] (Ryba, 1974) that can be used directly with the convex model approach in the present paper to calculate maximum vehicle responses. However, no expressions are given for the phase shifts between road input and vehicle responses. These expressions will be needed to calculate worst-road profiles of the type presented here.

The equation of motion for the 1-dof model is

$$m\ddot{y} + C\dot{y} + Ky = -m\ddot{\delta} \quad (7)$$

where  $\delta(t)$  is the motion from equation (6) that results from traversing road profile  $\delta(x)$  at velocity  $V$ , and  $y(t) = y_m(t) - \delta(t)$  is the relative displacement between the mass motion  $y_m(t)$  and the road surface. With

$$\omega^2 = K/m, \quad 2\zeta\omega = C/m \quad (8)$$

equation (7) becomes

$$\ddot{y} + 2\zeta\omega\dot{y} + \omega^2y = -\ddot{\delta} \quad (9)$$

where  $\omega$  is the undamped natural frequency of the system and  $\zeta$  is the fraction of critical damping from the viscous damper.

For  $\delta(t)$  we first find the solution for the  $n^{\text{th}}$  component of road roughness in equation (3), expressed as

$$\delta_n(t) = c_n \cos(\omega_n t + \beta_n) \quad (10)$$

where  $\omega_n = 2\pi nV/L$ . By straightforward solution of equation (9) with  $\delta(t)$  from equation (10), the steady-state solution for vehicle displacement relative to the road surface is found to be

$$y = \frac{c_n \Omega_n^2}{[(1 - \Omega_n^2)^2 + 4\zeta^2 \Omega_n^2]^{1/2}} \cos(\omega_n t + \beta_n - \alpha_{dn}) \quad (11)$$

where  $\Omega_n = \omega_n/\omega$  and the phase shift relative to the road input is

$$\alpha_{dn} = \tan^{-1} \frac{2\zeta\Omega_n}{1 - \Omega_n^2} \quad (12)$$

Steady-state vehicle acceleration (the vector sum of  $\ddot{y}$  and  $\ddot{\delta}$ ) is

$$\ddot{y}_m = c_n \omega_n^2 \left[ \frac{1 + 4\zeta^2 \Omega_n^2}{(1 - \Omega_n^2)^2 + 4\zeta^2 \Omega_n^2} \right]^{1/2} \cos(\omega_n t + \beta_n - \alpha_{an}) \quad (13)$$

with phase shift

$$\alpha_{an} = \tan^{-1}(2\zeta\Omega_n) \quad (14)$$

## THE CONVEX MODEL

Now, finally, the results of the preceding sections are put together with the concepts of convex modeling. A general treatise on convex models is given in [1] (Ben-Haim and Elishakoff, 1990). Models similar to the one that follows are developed in [6,7] (Lindberg, 1992a, 1992b). The general objective of a convex model is to obtain worst-case results for problems with input that is uncertain but bounded in some sense.

In the model used here the bound is taken such that the allowed range for each  $c_n^2$  has a variation with  $n$  as given by the power spectral density in equation (4). Thus

$$0 \leq c_n^2 \leq \kappa^2 n^{-2.5} \quad (15)$$

A method for determining the positive constant  $\kappa^2$  will be described later in this section. It is important to realize that this constant bears no relationship to the constant  $2kL^{1.5}$  in equation (4). The measured systematic variation of  $c_n$  with wavelength is used, but a convex model bound requires a separate bounding measurement.

Equation (15) is a consequence of the more general bounding specification that combinations of  $c_n$  will be taken such that they are bounded within an ellipsoid in  $c_n$  space. The ellipsoid is

$$\sum_{n=1}^{n=N} n^{2.5} c_n^2 \leq \kappa^2 \quad (16)$$

The ellipsoid extremes define the ranges given by equation (15), found by setting  $c_i = 0$  for  $i \neq n$  in expression (16). [For  $L > 100$  m, a constant coefficient value range  $0 \leq c_n^2 \leq \kappa^2 m^{-2.5}$  is used for the few modes with  $n < m = 0.01 L$ , corresponding to  $0 < \nu < 0.01$  in equation (1).]

It is now convenient to introduce vector representation for the road profile and vehicle responses. Then equation (6) becomes

$$\delta(t) = \sum_{n=1}^{n=N} c_n \cos(n\theta + \beta_n) \equiv \mathbf{D}^T \boldsymbol{\varphi} \quad (17)$$

where

$$\begin{aligned} \mathbf{D}^T &= \{c_1, c_2, \dots, c_N\} \\ \boldsymbol{\varphi}^T &= \{\cos(\theta + \beta_1), \cos(2\theta + \beta_2), \dots, \cos(N\theta + \beta_N)\} \end{aligned}$$

When a vehicle traverses a road described by equation (17), each wavelength of road roughness induces the steady-state responses given by equations (11) and (13). For maximum total response at time  $t$ , the modal responses must be in phase at this time. For pleasing display of results, this time is chosen as  $t = L/2V$ , which is when the vehicle is at the center of the length  $L$  and the circular test track coordinate is  $\theta = \pi$ . Thus, for maximum displacement at  $\theta = \pi$ ,  $\beta_n$  is chosen such that, in equation (11),  $\omega_n t + \beta_n - \alpha_n = 0$  at  $t = L/2V$ . With  $\omega_n t \equiv n\theta$  and  $\theta = \pi$  at  $t = L/2V$ , this gives

$$\beta_{dn} = \alpha_{dn} - n\pi \quad (18)$$

The argument of the cosine in equation (11) is then simply  $n(\theta - \pi)$ . With this, the total vehicle displacement is

$$y(\theta) = \sum_{n=1}^{n=N} c_n F_n \cos n(\theta - \pi) \quad (19)$$

where

$$F_n \equiv \frac{\Omega_n^2}{[(1 - \Omega_n^2)^2 + 4\zeta^2 \Omega_n^2]^{1/2}} \quad (20)$$

is the displacement response amplification function. In vector notation,

$$y(\theta) = \mathbf{D}^T \boldsymbol{\phi}_d \quad (21)$$

where

$$\begin{aligned} \boldsymbol{\phi}_d(\theta) &= \mathbf{F} \boldsymbol{\varphi}_\pi(\theta) \\ \mathbf{F} &= \text{diag}\{F_1, F_2, \dots, F_N\} \\ \boldsymbol{\varphi}_\pi^T &= \{\cos(\theta - \pi), \cos 2(\theta - \pi), \dots, \cos N(\theta - \pi)\} \end{aligned}$$

The subscript  $\pi$  denotes that  $\beta_{dn}$  have been chosen to give maximum displacement response at  $\theta = \pi$ , as described.

Proceeding in a similar way for acceleration response, the road surface roughness phase angles are taken as

$$\beta_{an} = \alpha_{an} - n\pi \quad (22)$$

The total acceleration is then

$$\ddot{y}(\theta) = \sum_{n=1}^{n=N} c_n G_n \cos n(\theta - \pi) \quad (23)$$

where

$$G_n \equiv \omega_n^2 \left[ \frac{1 + 4\zeta^2 \Omega_n^2}{(1 - \Omega_n^2)^2 + 4\zeta^2 \Omega_n^2} \right]^{1/2} \quad (24)$$

is the acceleration response amplification function. In vector notation,

$$\ddot{y}(\theta) = \mathbf{D}^T \boldsymbol{\phi}_a \quad (25)$$

where

$$\begin{aligned}\phi_a(\theta) &= \mathbf{G}\varphi_\pi(\theta) \\ \mathbf{G} &= \text{diag}\{G_1, G_2, \dots, G_n\}\end{aligned}$$

The expression for  $\delta(t)$  in equation (17) remains the same for the two problems, but the subscripts also denote that values for  $\beta_n$  are to be taken from equation (18) for maximum displacement and from equation (22) for maximum acceleration.

We can now more precisely define the convex model to be used. Two closely related sets of road roughness Fourier components  $c_n$  constitute the model: set  $R$  (range) of allowed coefficients and set  $E$  of extreme values of  $R$ . Thus, uncertainty in the road roughness profile is represented by allowing the roughness coefficient vector  $\mathbf{D}$  to vary on a convex set of values bounded within an ellipsoid:

$$R(\kappa, \mathbf{W}) = \{\mathbf{D} : \mathbf{D}^T \mathbf{W} \mathbf{D} \leq \kappa^2\} \quad (26)$$

which reads: set  $R$  is the set of all values of Fourier coefficients  $\mathbf{D}$  such that  $\mathbf{D}^T \mathbf{W} \mathbf{D} \leq \kappa^2$ . Here  $\mathbf{W}$  is an  $N \times N$  positive definite, real, symmetric matrix that specifies the shape of the ellipsoid in  $N$ -dimensional space, and  $\kappa^2$  is a positive number that specifies its size. In the present model,

$$\mathbf{W} = \text{diag}\{1^{2.5}, 2^{2.5}, \dots, N^{2.5}\}, \quad (27)$$

and the ellipsoid expression evaluates to expression (16).

Because vehicle responses are linear functions of  $c_n$ , and because  $R(\kappa, \mathbf{W})$  is a convex set (all convex combinations of its extreme points  $E$  are members of  $R$ , and these combinations completely map  $R$ ), the maximum response occurs on the set of extreme points  $E(\kappa, \mathbf{W})$ , given by

$$E(\kappa, \mathbf{W}) = \{\mathbf{D} : \mathbf{D}^T \mathbf{W} \mathbf{D} = \kappa^2\} \quad (28)$$

Maximum responses for displacement or acceleration are found by maximizing  $\mathbf{D}^T \phi$  subject to the constraint that  $\mathbf{D}$  is in the extreme-point set  $E$ . The following formalism is the same for either maximization, so we take  $\phi$  to represent either  $\phi_a$  or  $\phi_d$ . The desired maximum is found with the Hamiltonian

$$H = \mathbf{D}^T \phi + \lambda(\mathbf{D}^T \mathbf{W} \mathbf{D} - \kappa^2) \quad (29)$$

in which  $\mathbf{D}^T \phi$  is the function to be maximized and  $\lambda$  is a Lagrangian multiplier for the constraint. The extremum condition is

$$0 = \frac{\partial H}{\partial \mathbf{D}} = \phi + 2\lambda \mathbf{W} \mathbf{D} \quad (30)$$

To express  $\lambda$  in terms of  $\phi$  and  $\kappa$ , the symmetry of  $\mathbf{W}$  is first used to transpose the extremum condition:

$$\phi^T = -2\lambda \mathbf{D}^T \mathbf{W} \quad (31)$$

This expression is then post multiplied by  $\mathbf{W}^{-1}$  to obtain

$$\phi^T \mathbf{W}^{-1} = -2\lambda \mathbf{D}^T \quad (32)$$

Each side of this equation is post multiplied by the corresponding sides of the untransposed extremum condition (30) to give

$$\phi^T \mathbf{W}^{-1} \phi = 4\lambda^2 \mathbf{D}^T \mathbf{W} \mathbf{D} = 4\lambda^2 \kappa^2 \quad (33)$$

The desired expression for the Lagrange multiplier is then

$$\lambda = \pm \frac{1}{2\kappa} \sqrt{\phi^T \mathbf{W}^{-1} \phi} \quad (34)$$

The extremum condition is now premultiplied by  $\mathbf{D}^T$  to obtain

$$\mathbf{D}^T \phi = -2\lambda \mathbf{D}^T \mathbf{W} \mathbf{D} = \mp \kappa \sqrt{\phi^T \mathbf{W}^{-1} \phi} \quad (35)$$

The roughness coefficients that give this maximum response, from equations (30) and (34), is

$$\mathbf{D}_{\text{mr}} = \frac{\kappa \mathbf{W}^{-1} \phi}{\left[ \phi^T \mathbf{W}^{-1} \phi \right]^{1/2}} \quad (36)$$

The worst-road profile is

$$\delta_w(\theta) = \mathbf{D}_{\text{mr}}^T \varphi(\theta) \quad (37)$$

in which  $\varphi(\theta)$  is given by equation (17) with  $\beta_n$  from equation (18) or (22), as appropriate.

With  $\phi_d$  from equation (21), the maximum displacement response from equation (35) and  $\theta = \pi$  is

$$y_{\text{max}} = \kappa \left[ \sum_{n=1}^{n=N} n^{-2.5} F_n^2 \right]^{1/2} \quad (38)$$

Use of equation (37) with phase angles from equation (18) gives the worst-road profile for this displacement

$$\delta_d(\theta) = \frac{\kappa \sum_{n=1}^{n=N} n^{-2.5} F_n \cos(n\theta + \beta_{dn})}{\left[ \sum_{n=1}^{n=N} n^{-2.5} F_n^2 \right]^{1/2}} \quad (39)$$

With  $\phi_a$  from equation (25) and  $\theta = \pi$ , the maximum acceleration response is

$$\ddot{y}_{\text{max}} = \kappa \left[ \sum_{n=1}^{n=N} n^{-2.5} G_n^2 \right]^{1/2} \quad (40)$$

The road profile that gives this acceleration, with phase angles from equation (22), is

$$\delta_a(\theta) = \frac{\kappa \sum_{n=1}^{n=N} n^{-2.5} G_n \cos(n\theta + \beta_{an})}{\left[ \sum_{n=1}^{n=N} n^{-2.5} G_n^2 \right]^{1/2}} \quad (41)$$

These worst-road profiles should be avoided in road construction to the extent possible. The functional forms can also be used, along with a very simple road profile measurement, to obtain values for the constant  $\kappa$ . The measurement,  $\hat{\delta}$ , is simply half the difference between the highest and lowest points over a section of road of length comparable to the span of the worst-road profile (a distance corresponding to  $\theta$  ranging from the worst-road quiescent state, through its maximum, and back to the quiescent state). Then  $\kappa$  is chosen such that the peak of the worst-road profile is equal to this measured profile bound. Calculations in [6,7] (Lindberg, 1992a and 1992b) demonstrate that the resulting maximum vehicle responses are comparable to a  $3\sigma$  estimate of maximum response from a probabilistic model for road roughness with uncorrelated Fourier coefficients having a Gaussian distribution.

When  $\kappa$  is determined in this way, the peak of the maximum displacement response is

$$\frac{y_{\text{max}}}{\hat{\delta}} = \sum_{n=1}^{n=N} n^{-2.5} F_n^2 / \sum_{n=1}^{n=N} n^{-2.5} F_n \cos \alpha_{dn} \quad (42)$$

in which  $\theta = \pi$  was used in equation (39) to obtain the peak of the worst-road profile. The expression on the right is called the normalized maximum displacement. Proceeding in a similar way, the peak of the maximum acceleration response is

$$\frac{\ddot{y}_{\max}}{\hat{\delta}} = \sum_{n=1}^{n=N} n^{-2.5} G_n^2 / \sum_{n=1}^{n=N} n^{-2.5} G_n \cos \alpha_{an} \quad (43)$$

## NUMERICAL EXAMPLES

As a representative example, consider a vehicle with an undamped natural frequency of  $f = 1$  Hz. For this example it is found that it is sufficient to sum modes to  $f_N = 3$  Hz. A track length  $L = 400$  m then results in  $N = f_N L / V = 60$  modes for a vehicle velocity of  $V = 20$  m/s. The complete set of velocities considered is 10, 20, 30 and 40 m/s, which give 120, 60, 40 and 30 modes in the calculations, respectively. The mode number corresponding to  $\nu = 0.01$  in equation (1) is  $m = \nu L = 4$  for  $L = 400$  m. Calculations were also made for longer track lengths and higher cut-off frequencies  $f_N$  to demonstrate that results are essentially unchanged from those with the standard values just given.

A comprehensive set of results are given for road profiles that give maximum displacements and for profiles that give maximum accelerations, including the shape of the profiles that give these maxima and the resulting displacement or acceleration histories (plotted as functions of distance at constant vehicle velocity). These detailed results are given for damping ratios  $\zeta = 0.1, 0.2$  and  $0.5$ . Continuous curves of displacement maxima and acceleration maxima are given as functions of  $\zeta$  over a range from 0.1 to 1.0, with the above four velocities as a parameter.

### *Worst Roads for Vehicle Displacement*

Graphs of displacement amplification function  $F_n$  from equation (20) and phase angles  $\alpha_{dn}$  from equation (12) are given in Figures 1 and 2. These are familiar graphs that can be found in books on vibration. They are given here for completeness and to allow comparisons with the functions  $G_n$  and  $\alpha_{dn}$  for acceleration in the next subsection, which are not so generally available.

The worst-road profile for vehicle displacement with  $\zeta = 0.1$  is given in Figure 3, calculated with equation (39). In this and all the examples of detailed profiles and vehicle response, the vehicle velocity is 20 m/s. The most notable feature of this example is that, partly because of the small damping, the road profile is washboard-like at nearly the undamped natural frequency of the vehicle, ramping up very slowly to the track center where the vehicle experiences maximum displacement, and then ramping back down. At the track center there is a large spike of roughness, which might be called a resonant bump (or dip in the negative version).

Figure 4 is the worst-road profile for the same damping and vehicle velocity as in Figure 3 but with a track length of 400 m. Observe that this profile is identical to the central 400 m portion of the profile in Figure 3. Also note that in both graphs, and all that follow, if the graph were rolled around a cylinder the two ends would match to form a continuous curve. This is a consequence of the finite Fourier analysis and the reason it is helpful to visualize the interval  $0, L$  as a circular test track. Amplitudes in all the examples are normalized by  $\hat{\delta}$ ; the peak of the worst-road profile in length units is equal to  $\hat{\delta}$  (half the difference between the maximum and minimum road height measured on an actual road section).

Figure 5 is the vehicle response resulting from the road profile in Figure 4, found with equation (42) in its more general form with  $\cos n(\theta - \pi)$  in the numerator, from equation (19). Maximum displacement response in this case is about 2.6 times the peak of the road profile, that is,  $2.6 \hat{\delta}$ . Observe that, unlike the road profile, the response dies off quickly, and symmetrically, on each side of the maximum. A similar graph for the 800 m track length (not shown because of space limitations) demonstrates that the response is unchanged, that is, substantial response is limited to the central 200 m of the track, just as in Figure 5.

The dominant reason for the washboard appearance of the road profile in Figure 4 is that the phases between road input and response vary with wave number in an abrupt manner near vehicle resonance (see Figure 2). Thus, while all modes are in phase at the track center for response (by design of our maximizing procedure, to ensure maximum response at this location), they are not in phase for the road profile. Further, modal contributions cancel each other near the track "ends" much more quickly for response than for the road profile.

Figures 6 and 7 give corresponding results for  $\zeta = 0.2$ . The larger damping results in less of the washboard effect in the road profile, and vehicle response is even more concentrated near the track center. Finally, Figures 8 and 9 give results for  $\zeta = 0.5$ . Here the response is very abrupt but much reduced because of the larger damping (peak response is  $0.87 \hat{\delta}$  compared with  $2.6 \hat{\delta}$  for  $\zeta = 0.1$ ). Thus, with the substantial damping typical of usual vehicle suspension design, the worst-road profile and response tend toward a sudden dip or rise in the road.

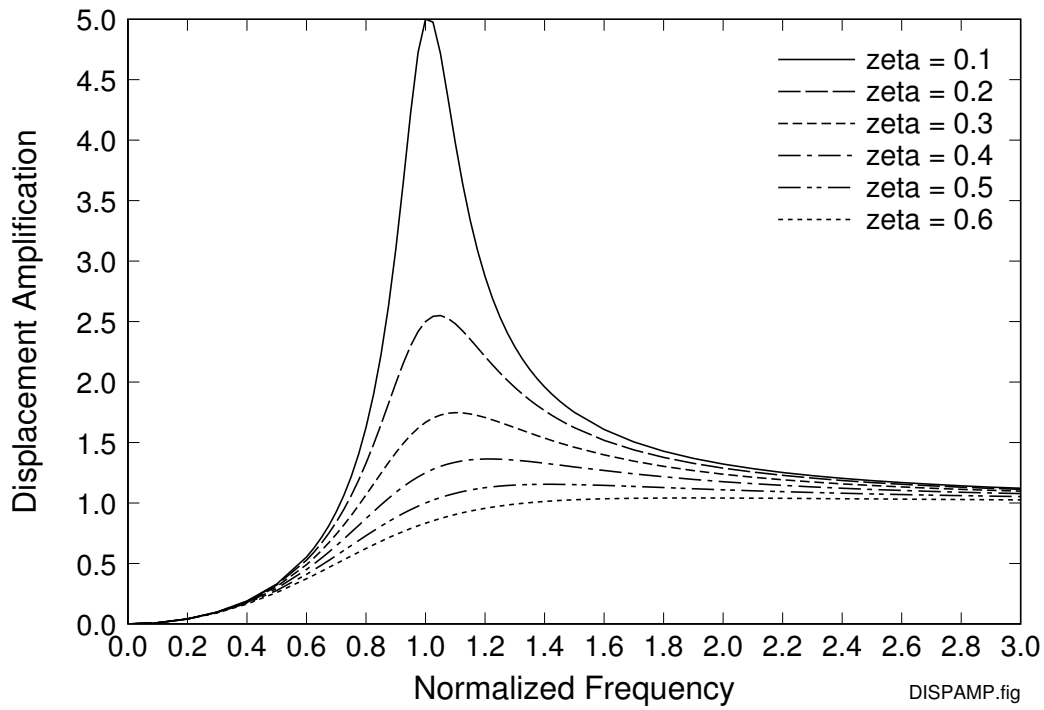


Figure 1. Displacement amplification  $F_n$  versus normalized frequency  $f_n/f$ .

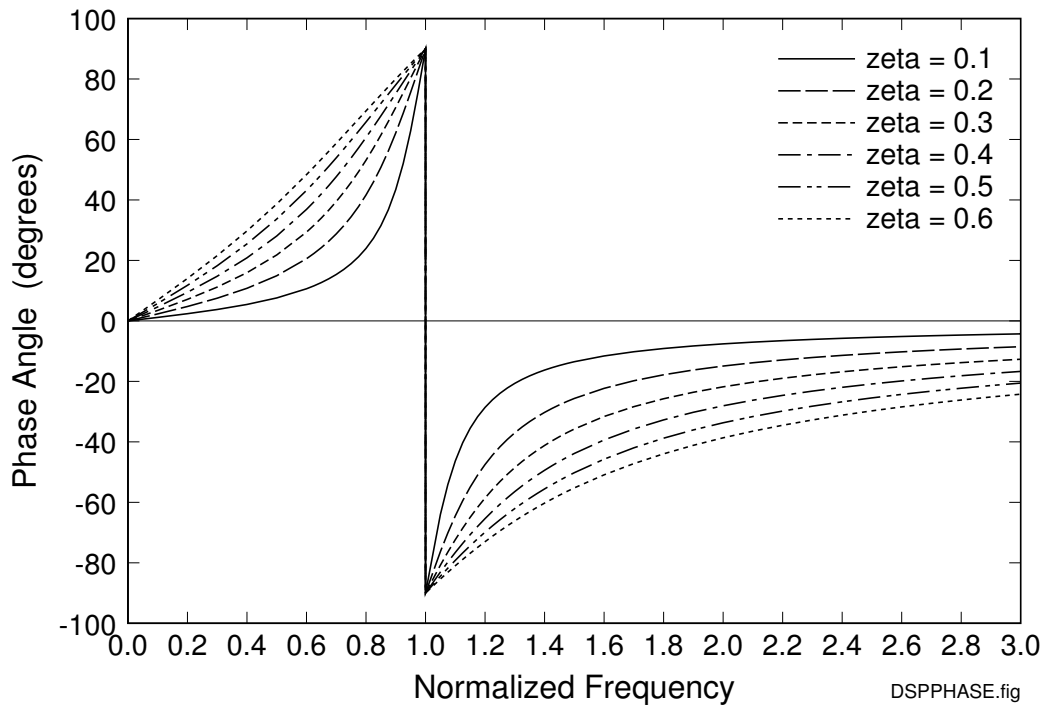


Figure 2. Phase angle  $\alpha_{dn}$  versus normalized frequency  $f_n/f$ .

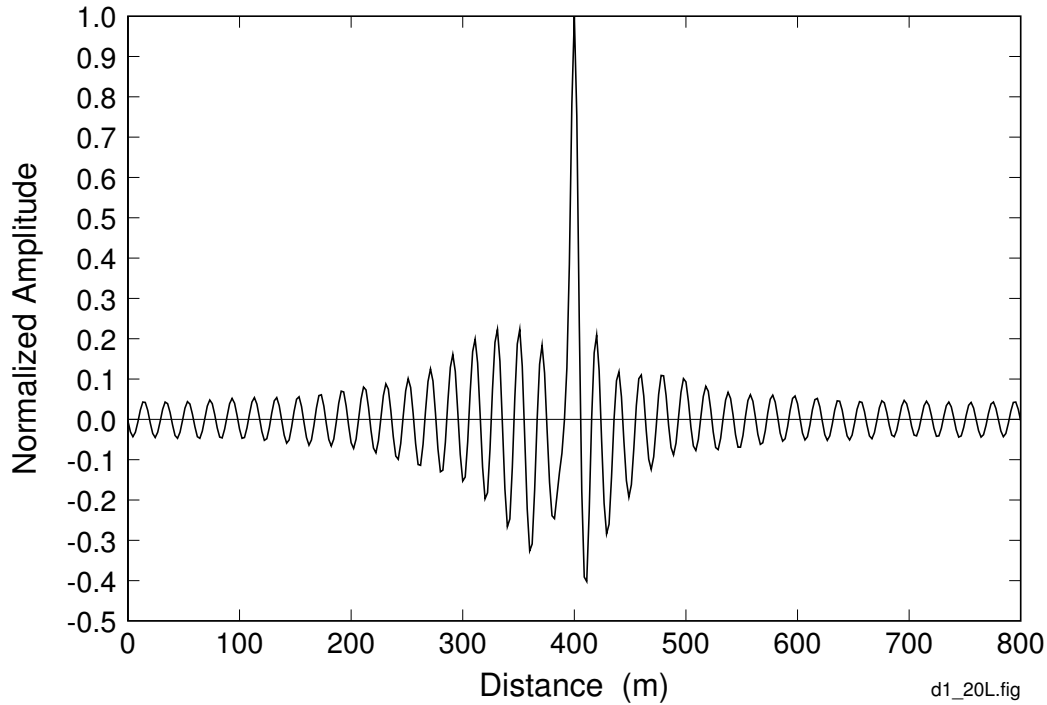


Figure 3. Worst-road profile for displacement;  $V = 20$  m/s,  $\zeta = 0.1$  and  $L = 800$  m.

Several calculations were made with  $F_N = 5$  Hz compared with the  $F_N = 3$  Hz chosen for all the results presented here. The results were essentially unchanged from those with  $F_N = 3$  Hz. Other calculations with velocities of 10, 30 and 40 m/s showed the expected change in road profile wavelengths, in proportion to velocity. Wave forms were essentially identical but at changed wavelengths (very small differences were caused by different low-mode constant  $c_n$  cut-off mode numbers  $m = 0.01 L$ , changed as  $L$  was adjusted in proportion to  $V$  to give the same graphs.) However, response amplitudes increased with increased velocity because of the larger amplitudes of road roughness coefficients at longer wavelengths, according to the Robson spectral function  $c_n^2 \propto n^{-2.5}$ .

This variation in response amplitude with  $V$  is given in Figure 10. Also shown is the monotonic decrease in amplitudes with increasing vehicle damping  $\zeta$ , for example from  $2.61 \hat{\delta}$  at  $\zeta = 0.1$  to  $0.55 \hat{\delta}$  at  $\zeta = 1$ , for  $V = 20$  m/s. This demonstrates why substantial damping is provided in vehicle suspension design. In the next subsection it will be shown that acceleration response does not vary monotonically with damping, and in fact has a minimum at about  $\zeta = 0.3$ . The minimum is flat enough that suspensions with  $\zeta = 0.5$ , or even somewhat larger, are reasonable to take advantage of the reduced vehicle displacement shown in Figure 10.

### **Worst Roads for Vehicle Acceleration**

Figure 11 gives the conventional graph of acceleration amplification (normalized by the base acceleration of the suspension spring) that one finds in vibrations texts, for example books on response to earthquakes. The unnormalized acceleration amplification, defined by  $G_n$  in equation 24, is given in Figure 12 for the  $\omega = 2\pi f = 6.28$  radians/s frequency of the  $f = 1$  Hz vehicle undamped natural frequency. Observe that, for small damping ratio  $\zeta$ , this amplification has the same general shape as the displacement amplification function  $F_n$  in Figure 1.

In contrast, the phase angles  $\alpha_{an}$  in Figure 13 for vehicle acceleration are distinctly different from those in Figure 2 for vehicle displacement. In particular, the phase curves in Figure 13 are continuous and have no sudden changes near the vehicle resonant frequency. This difference from Figure 2 results in distinctly different worst-road profiles for acceleration compared with worst-road profiles for displacement.

For example, compare the worst-road profile for acceleration in Figure 14 [calculated from equation (41)] with the corresponding profile for displacement in Figure 4, both with  $\zeta = 0.1$ . Because there is no phase angle discontinuity, the worst-road profile for acceleration does not have the washboard appearance of the profile for maximum displacement. Instead, it builds up from an essentially smooth road near  $x = 0$ , has a packet of waves

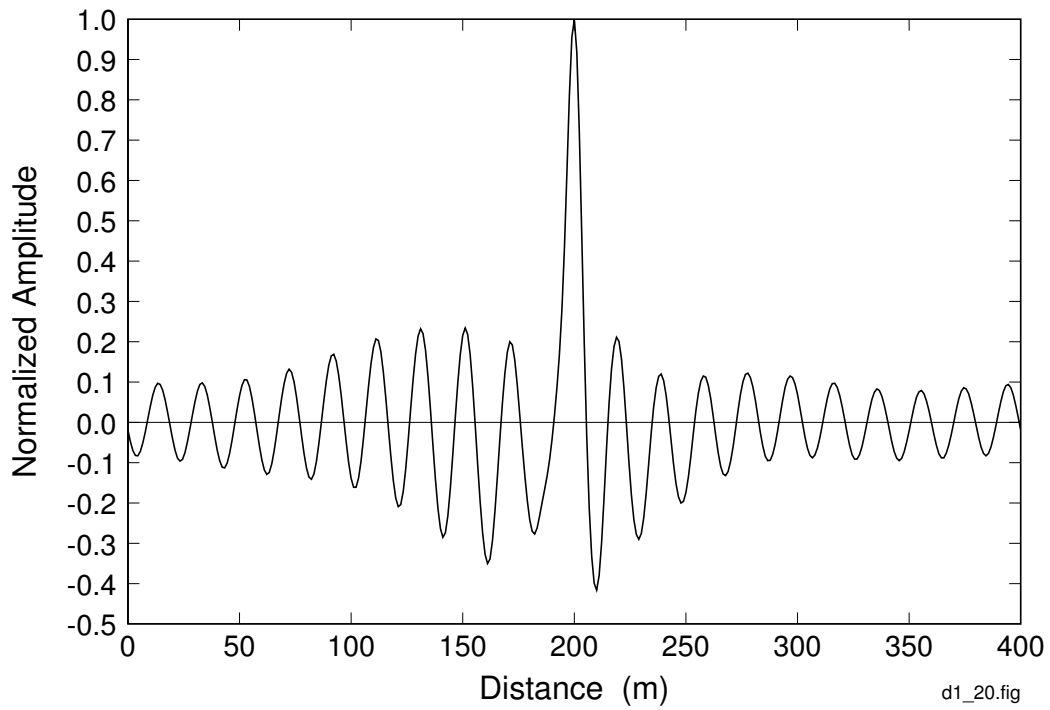


Figure 4. Worst-road profile for displacement;  $V = 20$  m/s,  $\zeta = 0.1$ , and  $L = 400$  m.

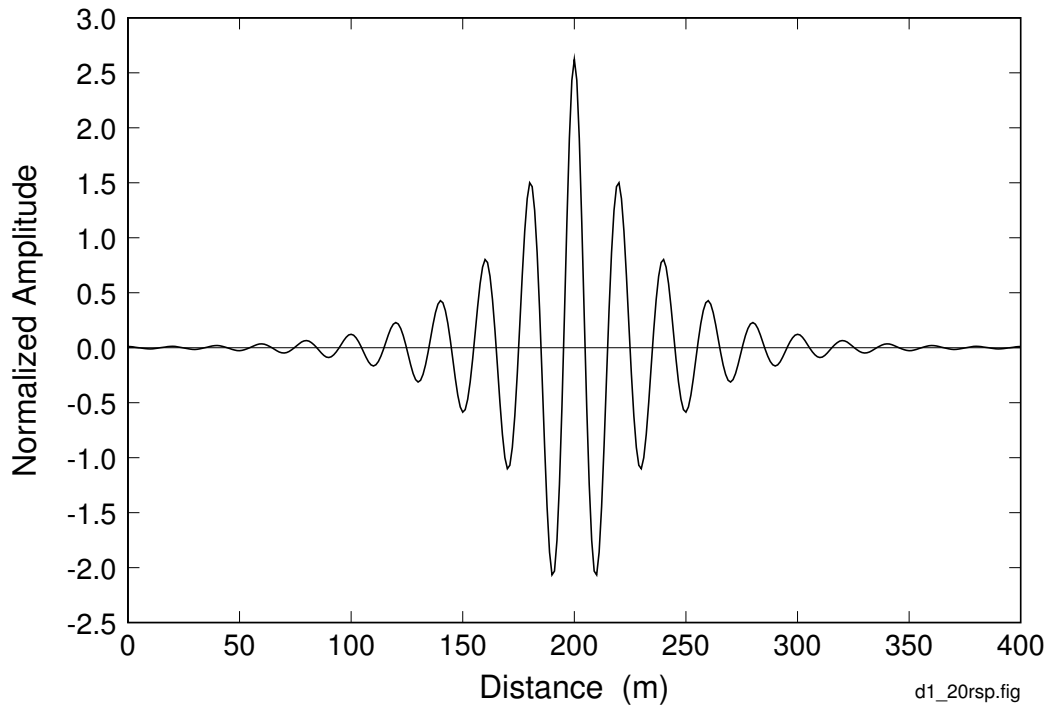


Figure 5. Vehicle displacement response to road profile in Figure 4.

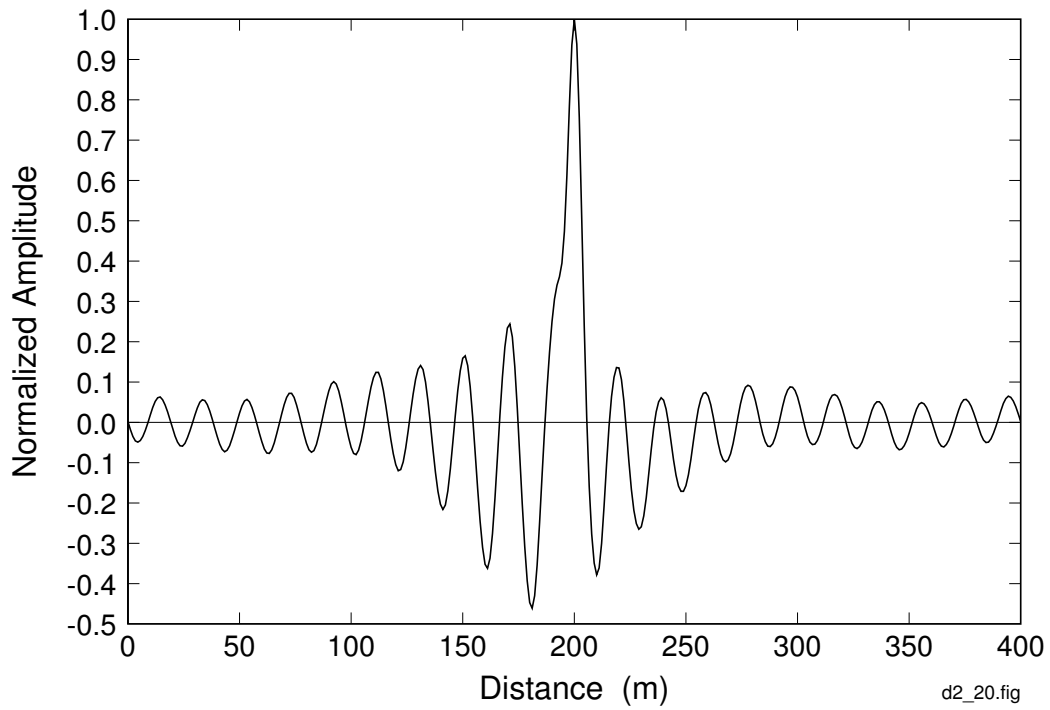


Figure 6. Worst-road profile for displacement with  $V = 20$  m/s and  $\zeta = 0.2$ .

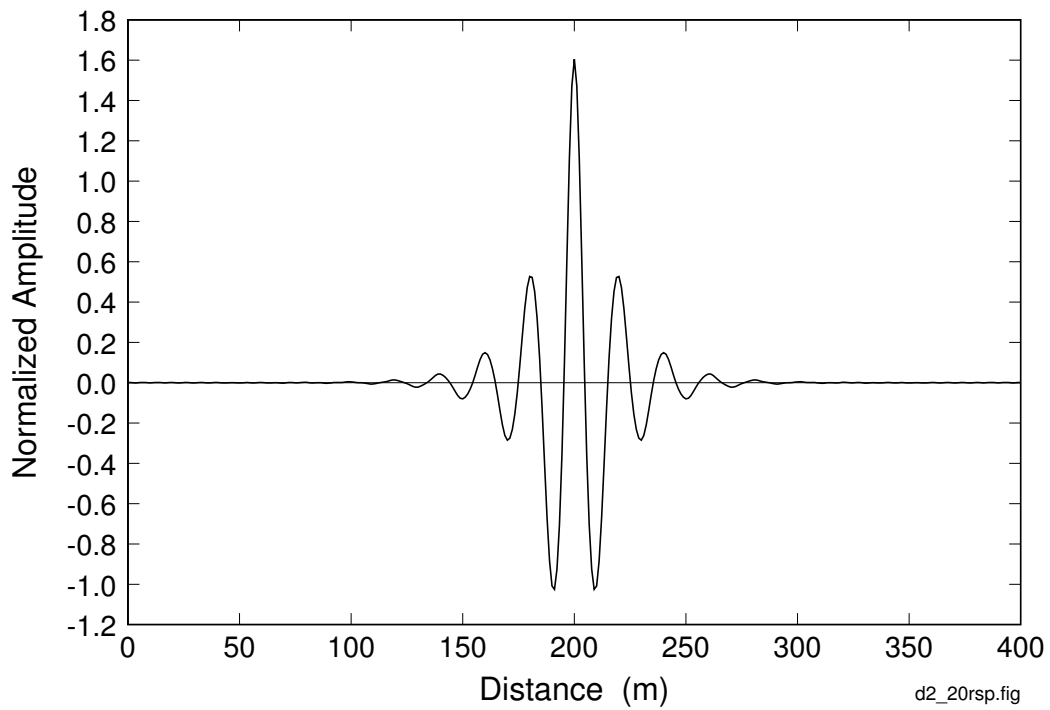


Figure 7. Vehicle displacement response to road profile in Figure 6.

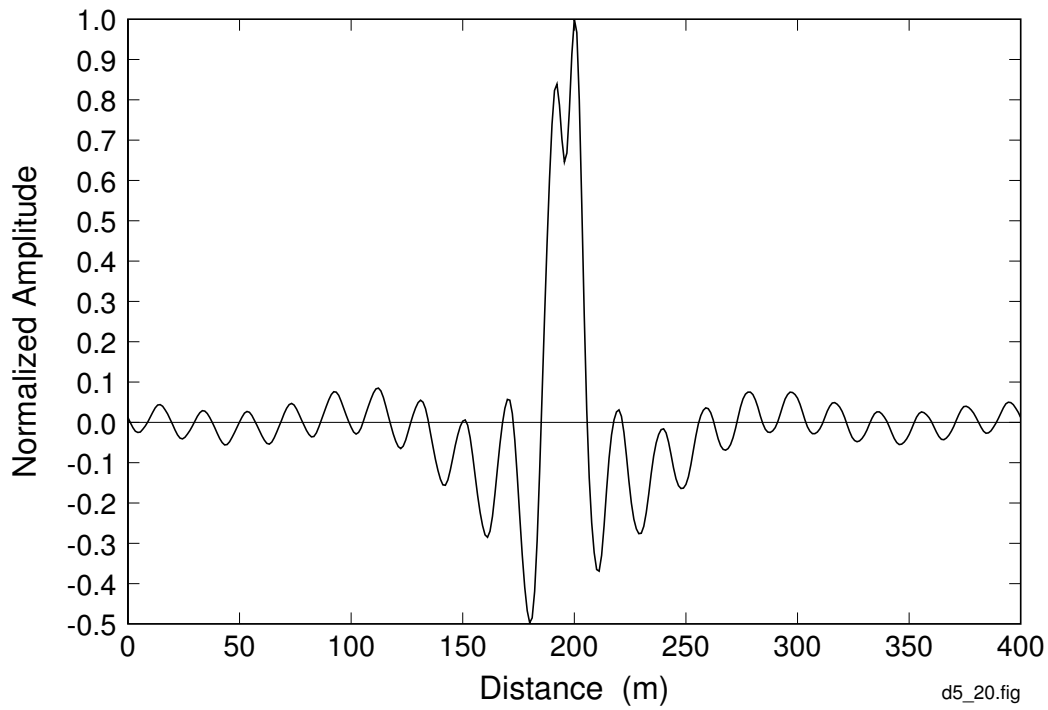


Figure 8. Worst-road profile for displacement with  $V = 20$  m/s and  $\zeta = 0.5$ .

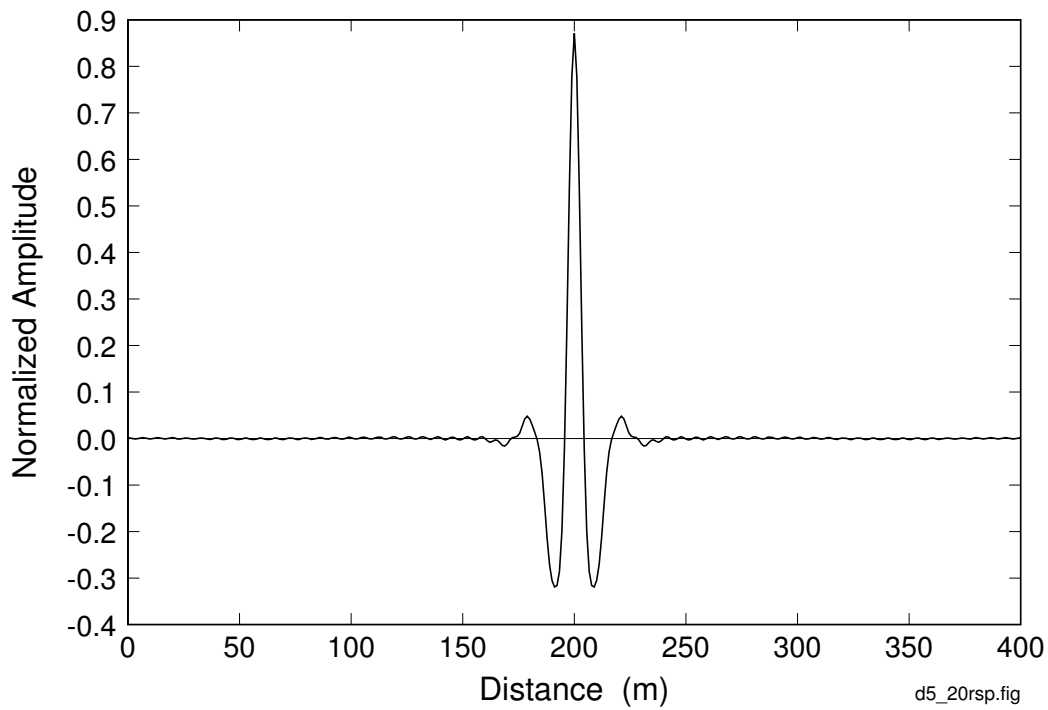


Figure 9. Vehicle displacement response to road profile in Figure 8.

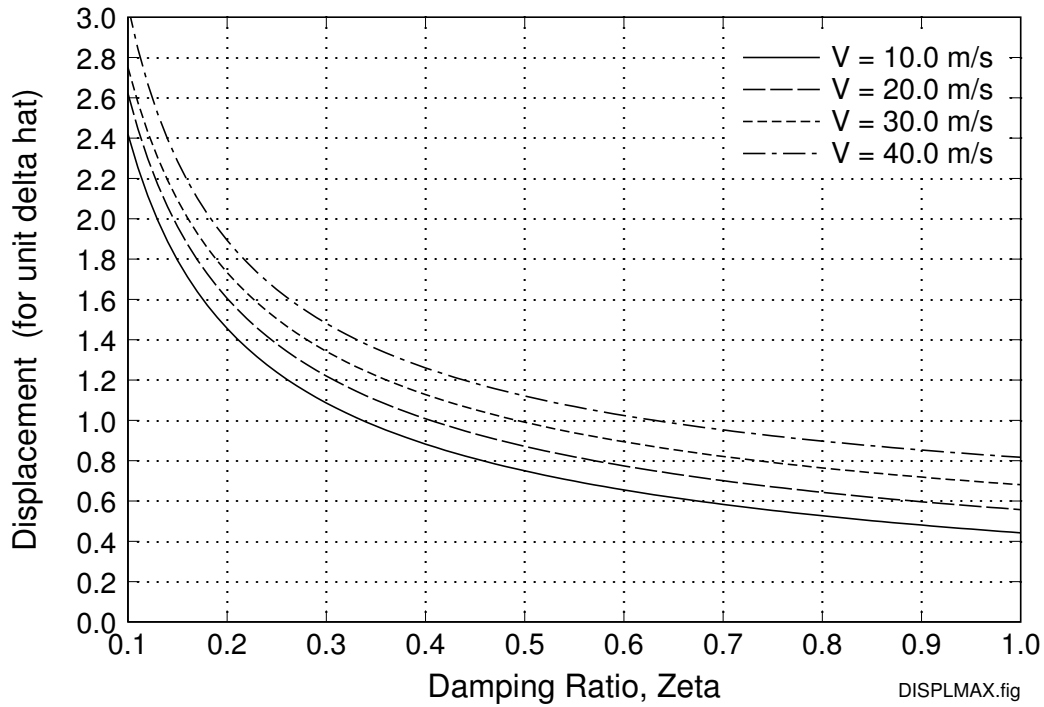


Figure 10. Vehicle displacement maxima versus  $\zeta$  for typical vehicle velocities (from 36 to 144 km/hr, about 22 to 90 mph).

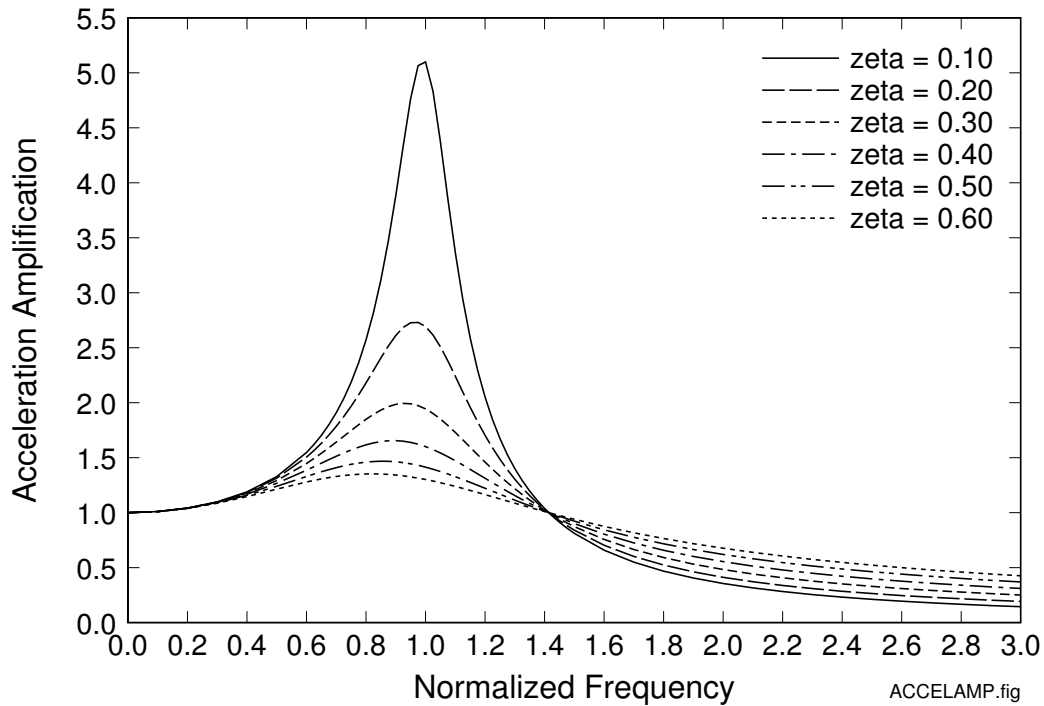


Figure 11. Acceleration amplification normalized to acceleration at the road surface (base of suspension spring).

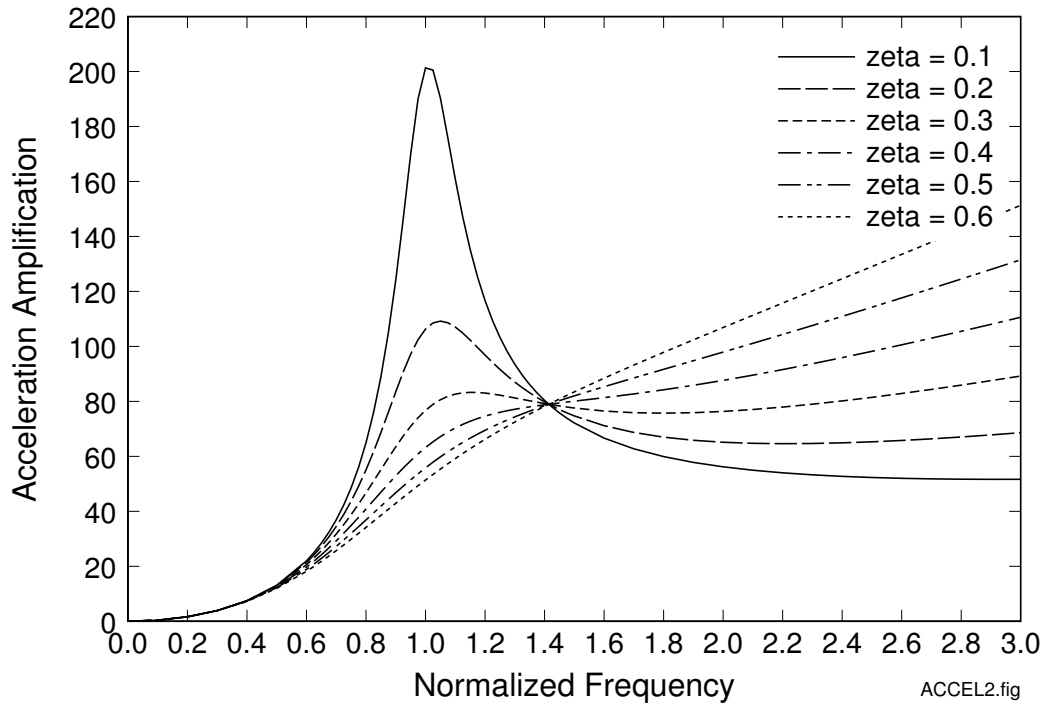


Figure 12. Acceleration amplification function  $G_n$  (in  $s^{-2}$ ) for  $f = 1$  Hz.

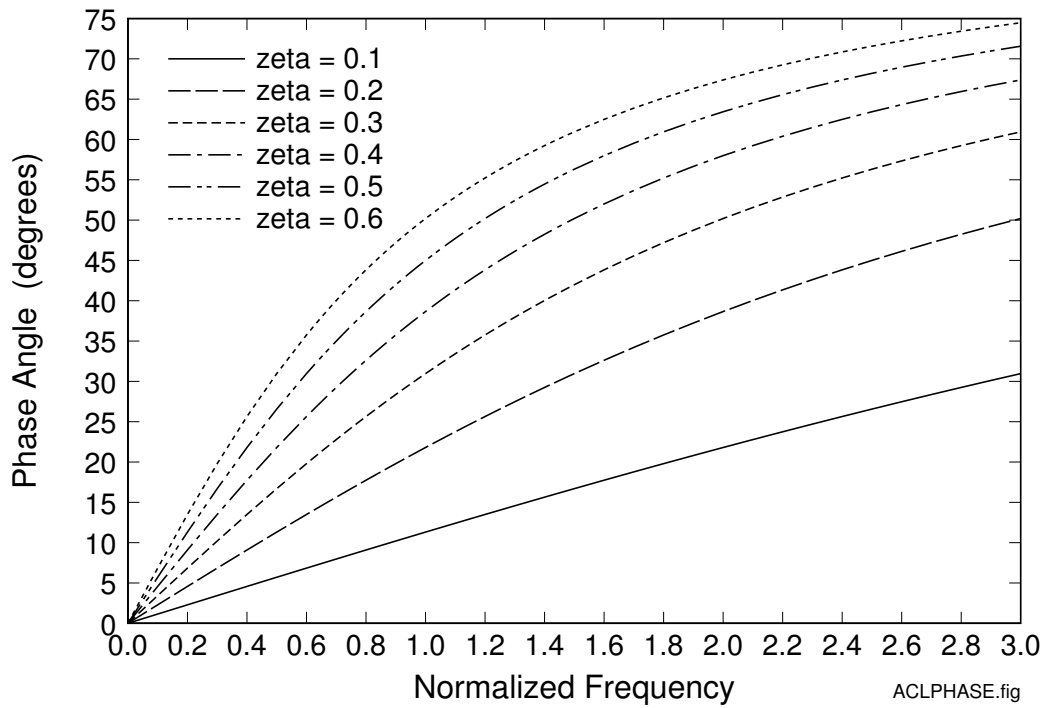


Figure 13. Phase angle  $\alpha_{an}$  versus normalized frequency  $f_n/f$ .

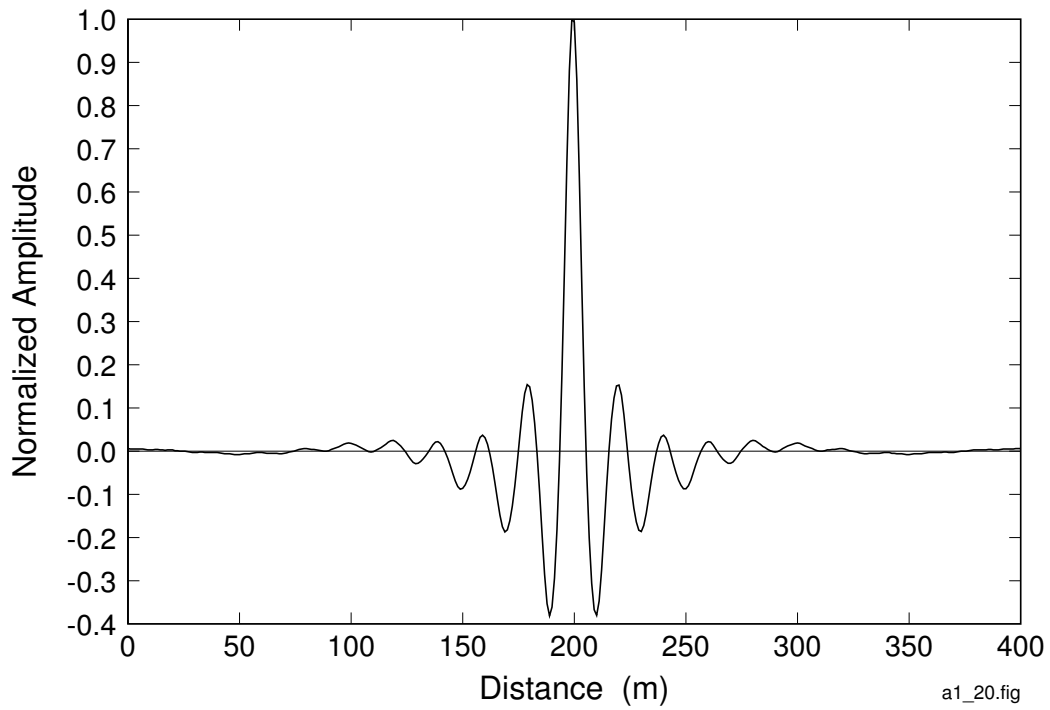


Figure 14. Worst-road profile for acceleration with  $V = 20$  m/s and  $\zeta = 0.1$ .

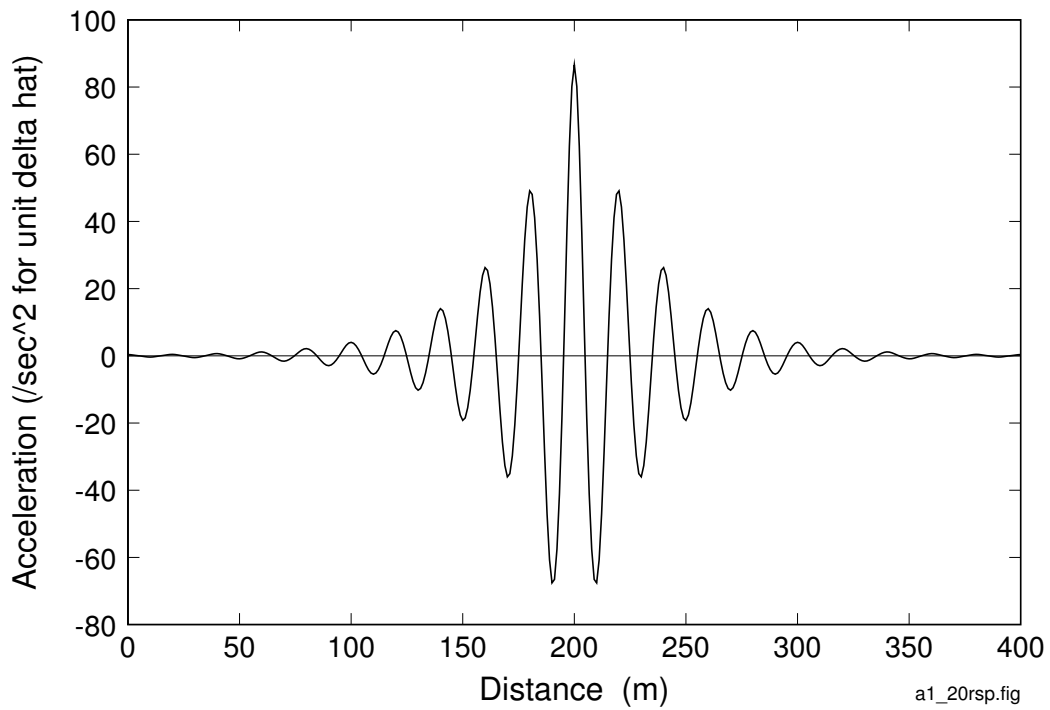


Figure 15. Vehicle acceleration response to road profile in Figure 14.

with rapidly varying amplitude centered on  $x = 200$  m, and then falls back to a smooth profile near the other end of the track, at  $x = 400$  m.

Acceleration response, in Figure 15 (calculated from equation (43) in its more general form with  $\cos n(\theta - \pi)$  in the numerator), has the same general character as the worst-road profile but builds up and decays more slowly. This is just the opposite from the profile/response behavior for displacement. Also observe that the response wave form for acceleration in Figure 15 is very nearly the same as that for displacement in Figure 5. This is a consequence of the similarity in amplification functions  $F_n$  in Figure 1 and  $G_n$  in Figure 11 for small  $\zeta$ . As already mentioned, by our maximization procedure modes are in phase at  $x = L/2$  for either maximum displacement or maximum acceleration, so response depends only on the amplification functions.

Worst-road profiles for acceleration and corresponding acceleration responses are given in Figures 16 and 17 for  $\zeta = 0.2$  and in Figures 18 and 19 for  $\zeta = 0.5$ . The results for  $\zeta = 0.2$  are similar to those for  $\zeta = 0.1$  except that the wave packets for both the road profile and response are more tightly grouped near the track center for the larger  $\zeta$ . For  $\zeta = 0.5$  the packing is so tight that the profile is essentially a bump with a dip on each side, and the response is mainly a single down, up and down acceleration burst. This character is similar to that for displacement response, except that the worst-road profile for displacement still has some of the washboard character for locations removed from the track center. The ripple in the worst-road profile for acceleration with  $\zeta = 0.5$  is at very short wavelengths, because of the rising amplification function  $G_n$  at high frequencies for  $\zeta = 0.5$  (see Figure 12).

Finally, graphs of maximum acceleration versus  $\zeta$  for several vehicle velocities are given in Figure 20. As mentioned, these have minima near  $\zeta = 0.3$ , demonstrating an optimum damping ratio to minimize acceleration response to worst-road profiles. Moderate increases in  $\zeta$  beyond 0.3, to take advantage of the continuously decreasing displacement maxima with increasing  $\zeta$  demonstrated in Figure 10, are advisable, but it is apparent that a substantial penalty in increased acceleration would result for damping ratios greater than about  $\zeta = 0.5$ . Ratios approaching  $\zeta = 1$  are definitely ill-advised.

Representative worst-road accelerations near the  $\zeta = 0.5$  compromise between reduced acceleration and reduced displacement are about  $70 \delta$  m/s<sup>2</sup> for these  $f = 1$  Hz examples. With  $\delta = 9800/70 = 140$  mm, maximum acceleration would be about 1g and the vehicle would leave the road surface, the limit of this analysis, which assumes continuous contact with the road.

To maintain a worst-road acceleration response less than, say, 0.2g would require  $\delta < 28$  mm, a small value. This would require that the total run-out of a road profile measurement be less than 56 mm over the approximately 150 m distance of significant amplitude in the worst-road profiles of Figures 14, 16 and 18. While this could be imposed as a road construction specification, it would be more reasonable to require that roughness shapes of the types in these figures be avoided, a more practical result than from a probabilistic estimate of worst-road response, which gives no information about the profiles that produce maximum responses. Because vehicles travel over a range of velocities, worst-road profiles at these velocities must also be avoided. These essentially scale in wavelength in proportion to vehicle velocity.

## CONCLUSIONS AND RECOMMENDATIONS

From these results it appears that convex modeling is a useful adjunct to the more conventional spectral response density analyses already established as a method for evaluating vehicle and human response to rough roads. The Fourier transform model presented here gives the road profiles that lead to undesirable response as well as maximum responses, and also guidance in vehicle suspension design to minimize response to such roads.

The central assumption in the present analysis is that the Robson spectral distribution of wave amplitudes results from the process-dependent characteristics of machines and methods used in road construction, and characteristics of road wear from vehicle transit and weathering. The worst-road profiles calculated here take into account these characteristic variations. Thus, it not unreasonable to expect that, given the random nature of process superposition, over some sections of roads the modal contributions will conspire to give undesirable responses of the types demonstrated here, unless waveform-specific precautions are taken during road construction and maintenance. Even with best efforts at such precautions, vehicles must be analyzed, designed, and tested to ensure satisfactory response to these extreme but not unrealistic environments.

It is recommended that this convex model analysis be extended to the quarter-car model that has served so well in spectral response density analyses. The foundations for such analysis have already been laid; it remains only to include phase information to calculate worst-road profiles. Also, the modal analysis machinery in finite element codes can be used to extend the Fourier convex model presented here to detailed analyses, including pitch, roll, vehicle body and seat vibrations, and human response.

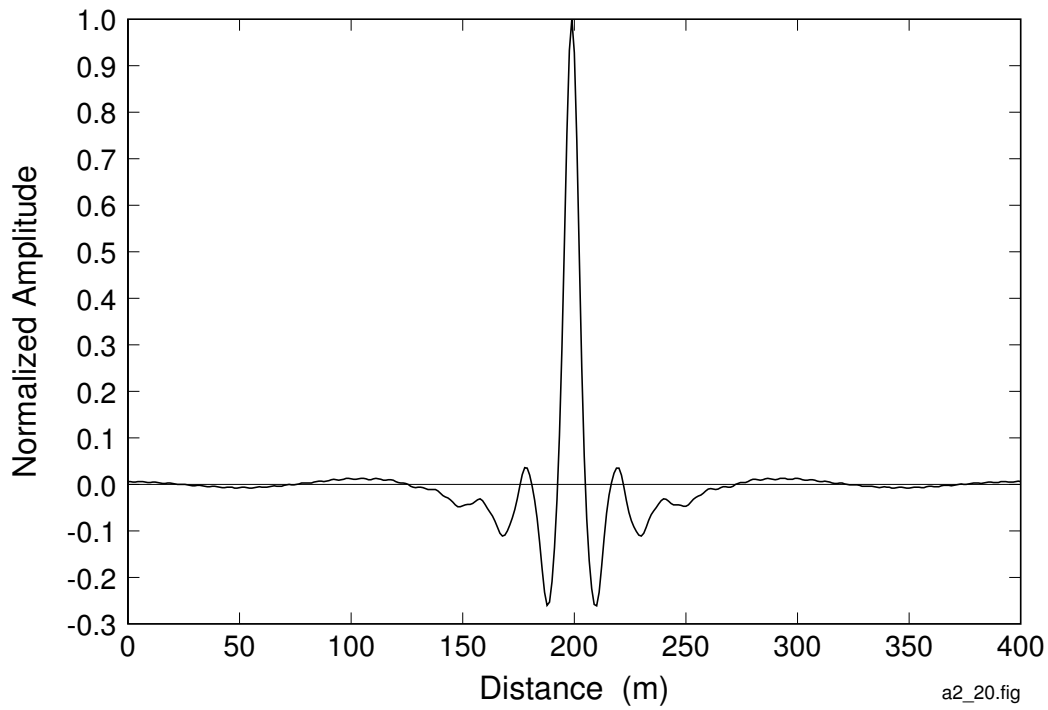


Figure 16. Worst-road profile for acceleration with  $V = 20$  m/s and  $\zeta = 0.2$ .

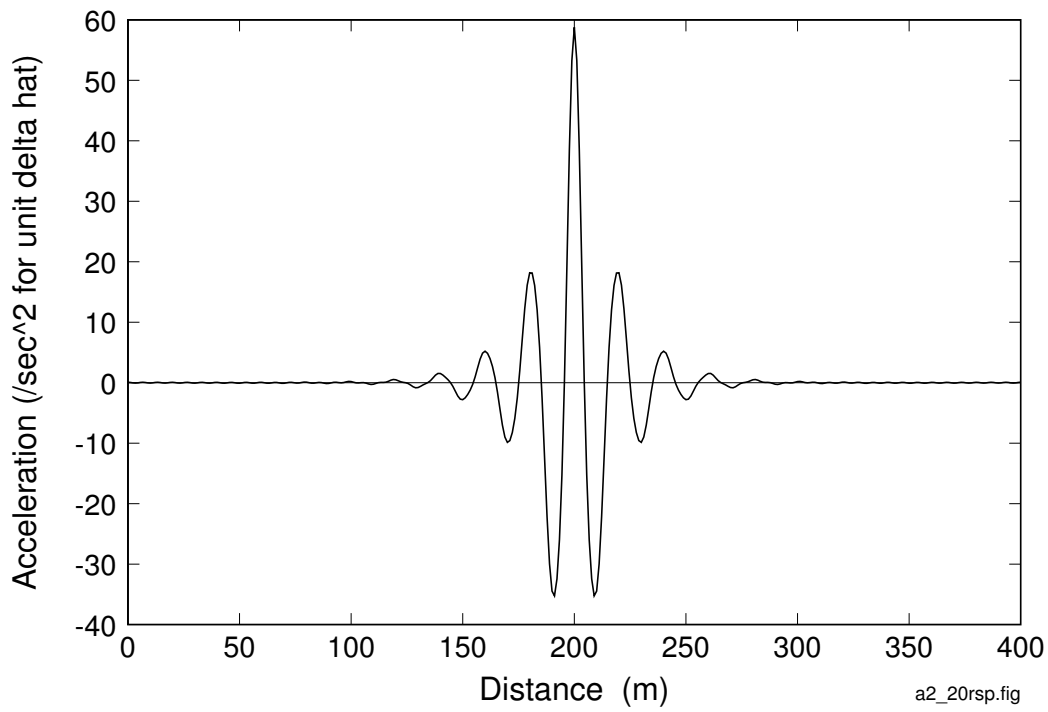


Figure 17. Vehicle acceleration response to road profile in Figure 16.

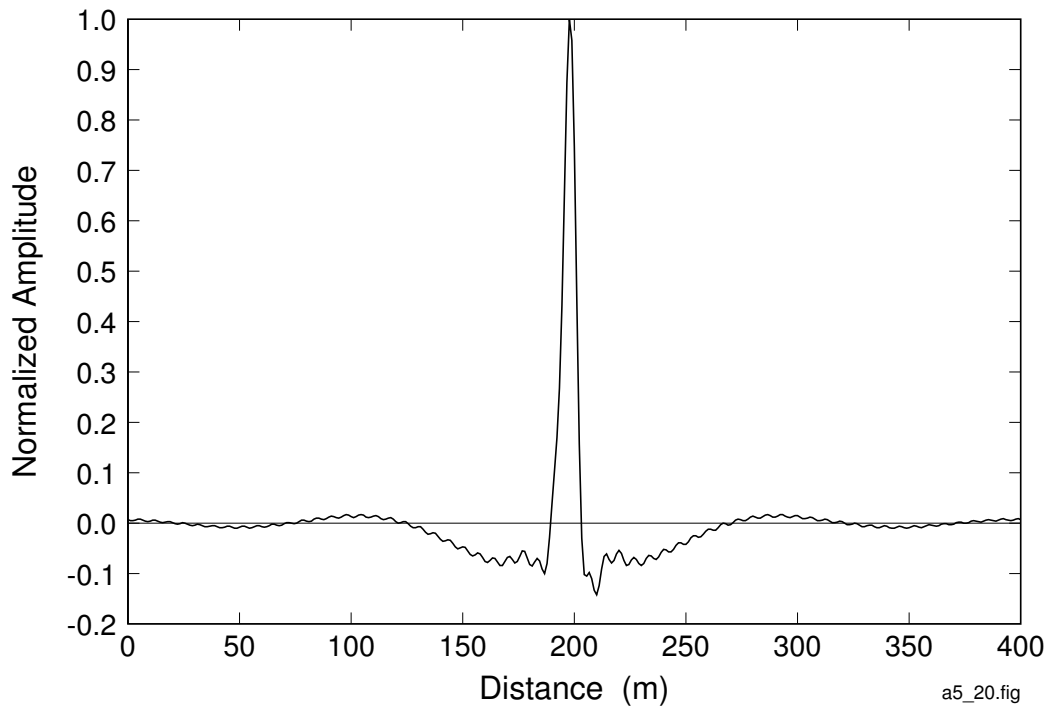


Figure 18. Worst-road profile for acceleration with  $V = 20$  m/s and  $\zeta = 0.5$ .

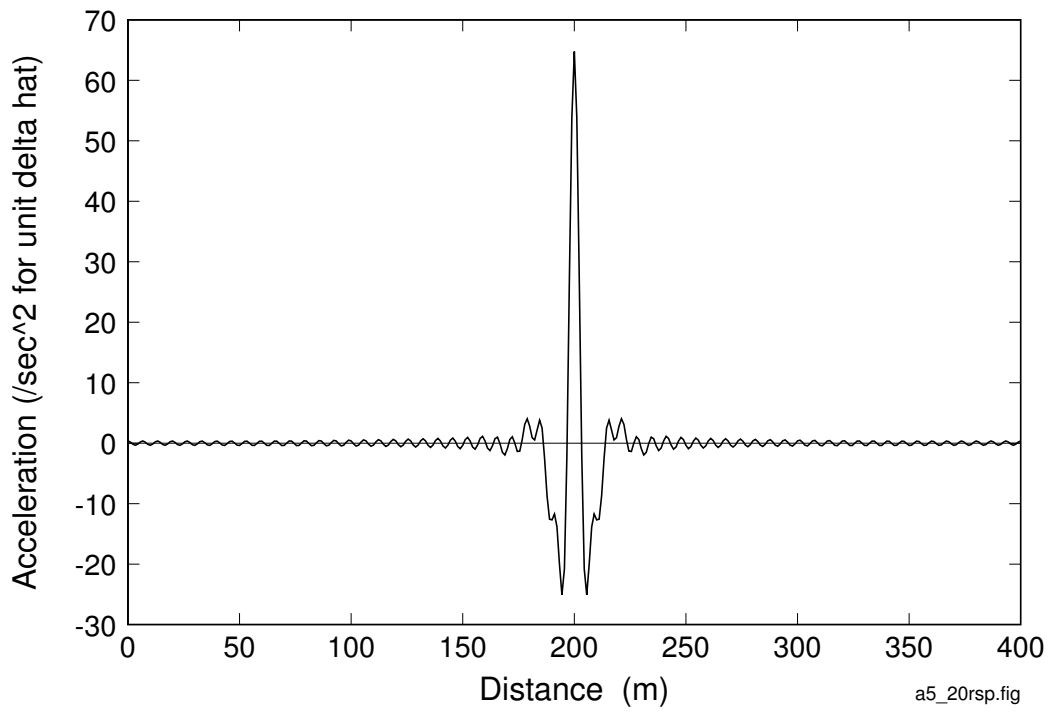


Figure 19. Vehicle acceleration response to road profile in Figure 18.

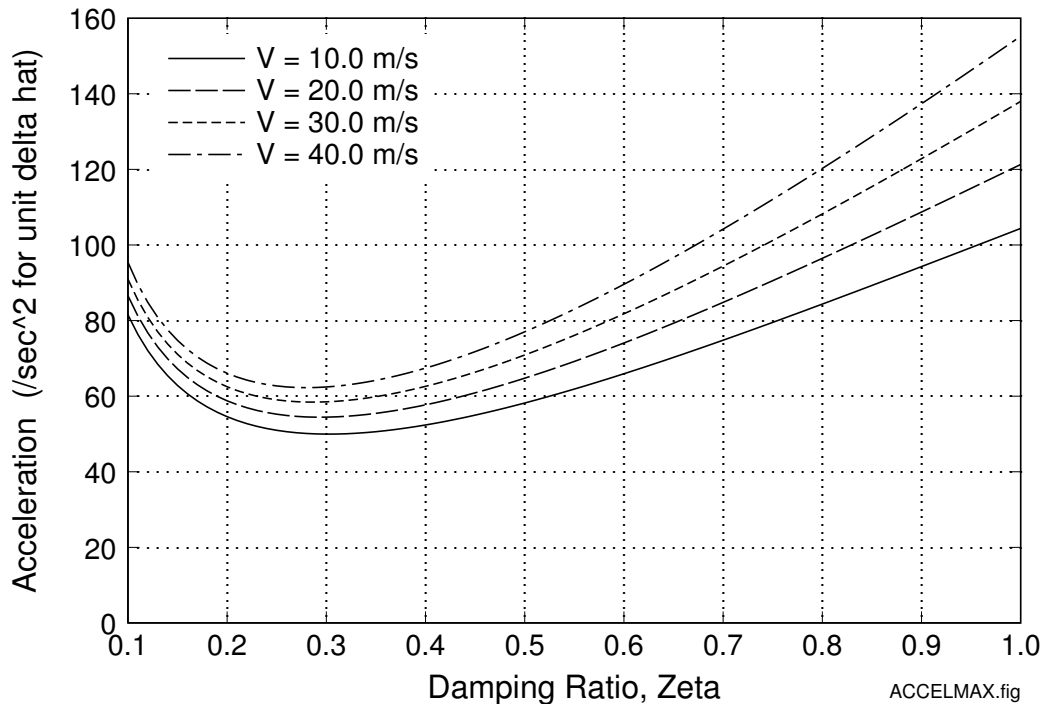


Figure 20. Vehicle acceleration maxima versus  $\zeta$  for typical vehicle velocities (from 36 to 144 km/hr, about 22 to 90 mph).

## REFERENCES

1. Ben-Haim, Y., and Elishakoff, I. (1990) *Convex Models of Uncertainty in Applied Mechanics*, Elsevier, New York.
2. Crolla, D. A., and Maclaurin, E. B. (1986) "Theoretical and Practical Aspects of the Ride Dynamics of Off-Road Vehicles—Part 2," *J. of Terramechanics*, Vol. 23, No. 1, pp. 1–12.
3. Dodds, C. J., and Robson, J. D. (1973) "The description of road surface roughness," *J. Sound Vibration*, vol. 31, pp. 175–183.
4. Hudson, W. R., et al (1983) "Root-Mean-Square Vertical Acceleration as a Summary Roughness Statistic," *Measuring Road Roughness and its Effects on User Cost and Comfort*, ASTM Symp., Bal Harbour, FL., Dec., 1983, ASTM Special Tech. Pub. 884, T. D. Gillespie and M. Sayers, ed., pp. 3–24.
5. ISO 2631, Revision Draft No. 5 (1983) *Guide to the evaluation of human exposure to whole-body mechanical vibration and repetitive shock*.
6. Lindberg, H. E. (1992a) "An Evaluation of Convex Modeling for Multimode Dynamic Buckling," *ASME J. of Appl. Mech.*, Vol. 59, pp. 929–936.
7. Lindberg, H. E. (1992b) "Convex Models for Uncertain Imperfection Control in Multimode Dynamic Buckling," *ASME J. of Appl. Mech.*, Vol. 59, pp. 937–945.
8. Robson, J. D. (1979) "Road surface description and vehicle response," *Int. J. of Vehicle Design*, vol. 1, no. 1, pp. 25–35.
9. Ryba, D. (1973) "Possible improvements in ride comfort," *Vehicle System Dynamics*, 2, pp. 1–32.
10. Ryba, D. (1974) "Improvements in Dynamic Characteristics of Automobile Suspension Systems," *Vehicle System Dynamics*, 3, pp. 17–46.
11. Sharp, R. S., and Crolla, D. A. (1987) "Road Vehicle Suspension Design — a Review," *Vehicle System Dynamics*, 16, pp. 167–192.
12. Sharp, R. S., and Aly Hassan, S. (1984) "The fundamentals of passive automobile suspension system design," *SEECO '84 Conference: Dynamics in Automotive Engineering*, Cranfield Inst. of Tech.
13. Van Deusen, B. D. (1968) "Human Response to Vehicle Vibration," *SAE Transactions*, paper 680090, pp. 328–345.